ACS APPLIED MATERIALS & INTERFACES

Research Article

www.acsami.org

pH- and Glucose-Responsive Core–Shell Hybrid Nanoparticles with Controllable Metal-Enhanced Fluorescence Effects

Jianfeng Zhang, Ning Ma,* Fu Tang, Qianling Cui, Fang He, and Lidong Li*

School of Materials Science and Engineering, University of Science and Technology Beijing, Beijing 100083, P. R. China

ABSTRACT: In this paper, a novel core–shell hybrid nanoparticle with a silver core and cross-linked poly(3-acrylamidephenylboronic acid-*co*-acrylic acid) shell (Ag@PAPBA-PAA) was reported. The prepared hybrid nanoparticles can exhibit good responsiveness to the glucose concentration and pH of the environment and exhibit a responsive swelling and shrinking behavior. Tuned by the glucose concentration or pH, a swelling of up to 15.0 nm thickness of the hybrid nanoparticle shell can be observed. These unique responsive properties can be employed to tune the metal-enhanced fluorescence (MEF) effects of the incorporated Ag cores. The fluorescence of adsorbed positively charged porphyrin molecules (Por^{4+}) shows good sensitivity to the glucose concentration and pH with an enhancement of up to about 1.8-fold. These functional hybrid nanoparticles with tunable MEF effects show a great potential application in the fields of responsive fluorescent sensing and detection.

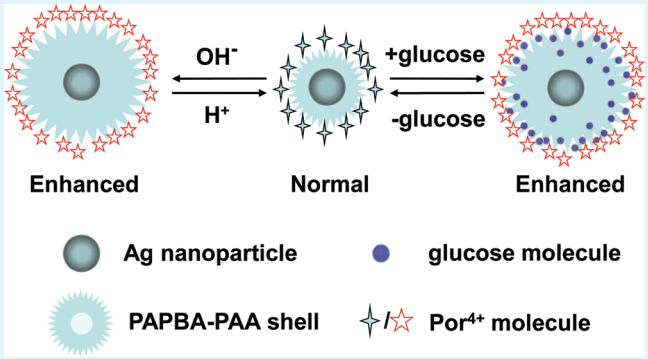

KEYWORDS: *self-assembly, fluorescence, metal-enhanced fluorescence, stimuli-responsive, nanoparticles*

INTRODUCTION

Fluorescence methods are an important class of technique in the fields of chemistry or biochemistry.[1−4] In some cases, many conventional fluorophores display weak fluorescence thus restricting their application for fluorescence detection and imaging. To overcome this shortcoming, the metal-enhanced fluorescence (MEF) detection method has been developed recently to further improve the fluorescence technique. The MEF effect is a phenomenon whereby fluorescent molecules in close proximity tunable metallic nanostructures (such as Ag, Au), display an increase in the fluorescence intensity.[5−8] This unique effect is due to the oscillating dipole of the fluorescence coupling with the plasmon resonance from the surface of the metal.[5] With the help of the MEF, the signal of the fluorescence can be greatly enhanced. The effect has been proven to increase the capabilities of fluorescence detection in the fields of chemistry or biochemistry.[9−12]

Among metallic nanostructures, Ag nanoparticles have attracted wide attention in MEF studies for their good MEF activity and their stability in solution.[13−17] Because the MEF effect is closely related to the interaction distance between the metal surface and the fluorescent molecules,[5] the fluorescence enhancement behavior of the system can be tuned by varying the distance between the two entities.[18−23] Therefore, core–shell hybrid nanoparticles with core of Ag nanoparticles and a shell of stimuli-responsive polymeric layers were prepared. Tunable MEF effects could then be realized by varying the metal–fluorophore distance due to the stimuli-responsiveness of the polymer shell.[15,16]

Among the external stimuli, glucose concentration is often studied due to the strong background of application in biological science. For glucose sensing, phenylboronic acid is considered to be an ideal glucose-recognition moiety and can reversibly bind with glucose by covalent bond formation to produce a negatively charged phenylboronate group.[24,25] This reversible binding behavior makes phenylboronic acid a good candidate for the design of glucose-responsive systems.

In this paper, we prepared a novel hybrid nanoparticle by synthesizing a pH- and glucose-sensitive poly(3-acrylamidephenylboronic acid-*co*-acrylic acid) (PAPBA-co-PAA) polymeric shell around the Ag nanoparticle core, and then adsorbing Por^{4+} fluorescence entities onto the surfaces of the core–shell Ag@PAPBA-PAA nanoparticles. As shown in scheme 1, the distance between the Ag cores and the fluorescent molecules can be controlled, and correspondingly, the responsive MEF behavior of the Por^{4+}/Ag@PAPBA-PAA nanocomposite can be realized.

EXPERIMENTAL SECTION

Materials. *N*,*N*′-Bisacryloylcystamine (BAC) and 5,10,15,20-tetrakis-(1-methyl-4-pyridyl)-21*H*,23*H*-porphine, tetra-*p*-tosylate salt (Por^{4+}) were purchased from Sigma Aldrich. 3-Aminophenylboronic acid (98%, monohydrate), acrylic acid (AA), azobisisobutryonitrile (AIBN), and other chemicals and solvents were purchased from Beijing Chemical Reagent Co. Ltd..

Received: December 30, 2011
Accepted: February 10, 2012
Published: February 10, 2012

dx.doi.org/10.1021/am201858u | *ACS Appl. Mater. Interfaces* 2012, 4, 1747–1751

Scheme 1. Schematic Illustration of the pH- and Glucose-Responsive Swelling-Shrinking Behavior of the Ag@PAPBA-PAA Hybrid Nanoparticles and the Corresponding Controllable MEF Effects

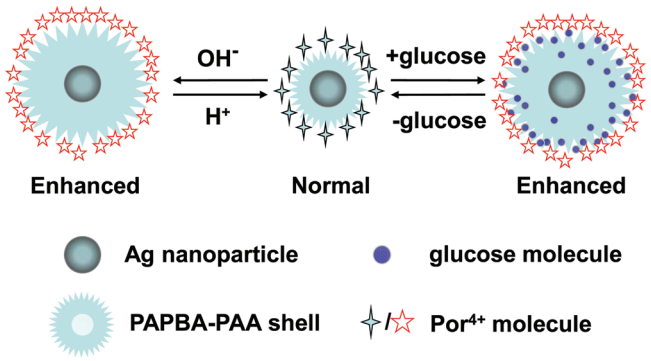

Instrumentation. The morphologies of the hybrid nanoparticles were observed using a JEM-2010 transmission electron microscope with an accelerating voltage of 120 kV; the sample was stained with 0.2% phosphotungstic acid hydrate before observation. The size distribution of the hybrid nanoparticles was determined with a Malvern NS 90 Zetasizer using a monochromatic coherent He−Ne laser (633 nm) as the light source, and a detector that monitored the light scattered at a 90° angle. Metal enhanced fluorescence studies were performed on a Hitachi F-7000 spectrofluorometer. The maximum surface plasmon absorption of prepared Ag nanoparticles was determined with a Hitachi U3900 spectrophotometer.

Synthesis of 3-Acrylamidephenylboronic Acid (APBA). The glucose-responsive monomer APBA was synthesized according to the reported procedure.[24] Two and a half grams of 3-aminophenylboronic acid was dissolved in 50 mL of aqueous sodium hydroxide solution (5.0 wt %) and cooled in an ice bath for 10 min. Then, 2.0 mL acryloyl chloride was added dropwise into the above solution over a period of 10 min. The reaction mixture was kept for 3 h in room temperature. After that, the pH of the solution was adjusted to 7.0 with dilute hydrochloric acid (0.1 M) whereupon a gray precipitate appeared. The precipitate was washed with deionized water and extracted with ethyl acetate twice, resulting in a gray powder, obtained with a yield of 76% after rotary evaporation and vacuum drying. ^{1}H NMR (300 MHz, $CDCl_3$) δ (ppm): vinyl protons: 6.46 (1H, t), 6.23 (1H, d), 5.77 (1H, d); aromatic protons: 7.99 (1H, d), 7.70 (1H, d), 7.56 (1H, d), 7.37 (1H, t).

Preparation of Ag@PAPBA-PAA Hybrid Nanoparticles. Ag nanoparticles were prepared by a method of tannic acid reduction and vinyl functionalized by the introduction of BAC.[26] The PAPBA-PAA shell was fabricated onto the vinyl-rich Ag nanoparticles via a free radical polymerization step. First, the vinyl functionalized Ag nanoparticles were obtained by adding 50 μL of the prepared Ag nanoparticles to 5.95 mL BAC in ethanol solution (0.60 mg/mL) under vigorous stirring at 700 rpm. The total volume of the mixture was 6 mL and the reaction was allowed to proceed for 24 h at room temperature. APBA in ethanol solution (500 μL, 7.20 mg/mL) and AA in ethanol solution (50 μL, 63.00 mg/mL) were then added to the mixture under argon. After 30 min, the argon flow was stopped and the polymerization was initiated by the injection of AIBN in ethanol solution (250 μL, 1.97 mg/mL). The polymerization was allowed to proceed at 70 °C for 2 h. To remove some silver-free particles as well as oligomers and unreacted monomers, the core−shell hybrid nanoparticle dispersion obtained was diluted with deionized water (6 mL), purified by centrifugation and washing with deionized water three times, and finally redispersed in 1.2 mL of water for further experiments.

Responsive Behavior of the Hybrid Nanoparticles. The size distribution and the responsive behavior of the Ag@PAPBA-PAA nanoparticles were observed by the dynamic light scattering (DLS) method. For the glucose-response experiments, the size of the nanoparticle was tuned by gradually adding an aqueous glucose solution (1.0 M) into the 1.2 mL of nanoparticle dispersion in phosphate-buffered saline (PBS) buffer solution.[27] For the pH-response experiments, a pH range of 4−10 was investigated, which was achieved by adding NaOH or HCl in aqueous solution.

Responsive MEF Studies. A solution of Por^{4+} was prepared by adding 20 μL Por^{4+} (3.0×10^{-6} M) to 1.0 mL PBS buffer solution (pH 9.0). The fluorescence spectra of Por^{4+} solution without Ag@PAPBA-PAA nanoparticles was first recorded with an excitation at 417 nm. Then, 20 μL of the Ag@PAPBA-PAA hybrid nanoparticle solution was added to the Por^{4+} solution and the fluorescence intensity measured after an incubation period of 30 min. During this period, the Por^{4+} ions were assembled onto the surface of the Ag@PAPBA-PAA, forming the nanocomposite of Por^{4+}/Ag@PAPBA-PAA. The mechanism of the Por^{4+} assembly was mainly based on the electrostatic interactions. The MEF behavior of the nanocomposite was tuned by adding glucose solution or adjusting the pH of the solution, and monitored by fluorescence spectroscopy. The enhancement factor was calculated by comparing the fluorescence intensity at 650 nm of the hybrid nanoparticle with added Por^{4+} solution and that of the pure Por^{4+} solution obtained under the same measurement conditions.

RESULTS AND DISCUSSION

The spherical Ag nanoparticles were synthesized by a tannic acid reduction method, with an average diameter of 23 ± 3 nm, as shown in Figure 1a. The maximum surface plasmon absorption was determined as 417 nm by UV−vis spectroscopy. The PAPBA-PAA shell was prepared on vinyl-modified Ag nanoparticle surfaces by a simple free radical polymerization of APBA and AA in aqueous solution. Before the polymerization, *N*,*N*′-bisacryloylcystamine (BAC) was used to introduce vinyl groups onto the surface of the Ag nanoparticles because of the strong affinity between Ag and disulfide groups. At the same time, BAC also acted as the cross-linker and copolymerized

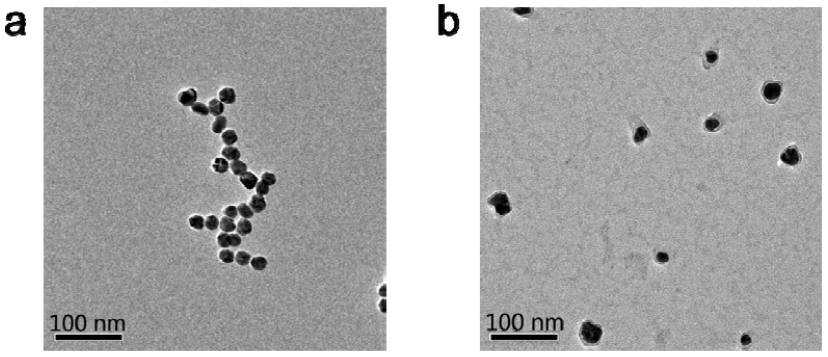

Figure 1. TEM images of (a) pure Ag colloids and (b) Ag@PAPBA-PAA hybrid nanoparticles.

with APBA and AA during the polymerization with AIBN as a radical initiator. During the polymerization, the PAPBA-PAA polymer chains grew onto the Ag nanoparticles and formed uniform cross-linked polymeric shells in the presence of the BAC cross-linker. The swelling−shrinking properties of the micro/nanogel system were greatly dependent on the level of cross-linking. It is understandable that a higher degree of cross-linking can result in a lower swelling ratio of the micro/nanogel.

In this work, the amount of BAC cross-linker was relatively high compared with that of the monomer (the ratio of BAC to APBA monomer is about 1:4) and this was used to realize a strong cross-linking and ensure a proper thickness of the polymer shell for operation of the MEF effect. Since the MEF is quite sensitive to the interaction distance between Ag nanoparticles and fluorophores, we needed to prepare hybrid nanoparticles in which the shell thickness increased gradually. The sizes of the hybrid nanoparticles were about 38 nm. Since the size of the Ag core is about 23 nm, it indicates that the polymer shell of the nanoparticles were about 7.5 nm. This is a well-matched thickness for the appropriate interaction distance for MEF effects, as reported that optimal distance located in the range of 5−20 nm.[5]

For comparison, we also prepared Ag@PAPBA-PAA nanoparticles with thicker polymeric shells by using a smaller amount of BAC (BAC:APBA = 1:8). The obtained hybrid nanoparticles showed a shell thickness of about 28.5 nm and were employed to investigate the MEF behavior. It is found that the obtained hybrid nanoparticles showed almost no MEF enhancement for Por^{4+} molecules, indicating that a shell thickness of 28.5 nm had exceed the optimal distance of MEF effects.[5] For this reason, the former hybrid nanoparticles were selected for further MEF studies. The structure of the Ag@PAPBA-PAA nanoparticles was also observed by TEM. From the image of Figure 1b, we can see that the Ag@PAPBA-PAA nanoparticles show good core−shell structures. The average size of the Ag@PAPBA-PAA nanoparticles is about 40 nm, which is in good accordance with the size measured by DLS. It should be mentioned that in the polymerization process, the amount of Ag nanoparticles in the monomer solution was controlled at a low level (50 μL, 0.7 mg/mL) to avoid the cross-linking or aggregation of the obtained hybrid nanoparticles.

The APBA moieties in the hybrid nanoparticles are glucose-sensitive and can react reversibly with 1, 2-*cis*-diols such as glucose. The binding with glucose makes the APBA groups adopt a highly charged form. So the degree of ionization on the hydrogel modified with the APBA group increases and builds up a Donnan potential leading to hydrogel swelling behavior,[28] as can be seen in Scheme 2. On the basis of this mechanism,

Scheme 2. Complexation Equilibria between the Phenylboronic Acid Derivative and Glucose

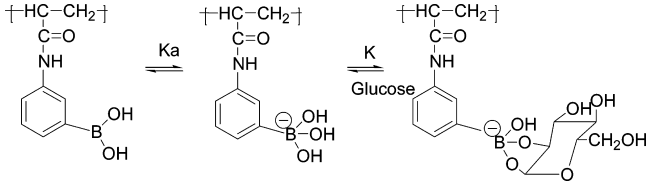

Ag@PAPBA-PAA hybrid nanoparticles exhibit a good glucose-responsive swelling behavior. As shown in Figure 2a, the

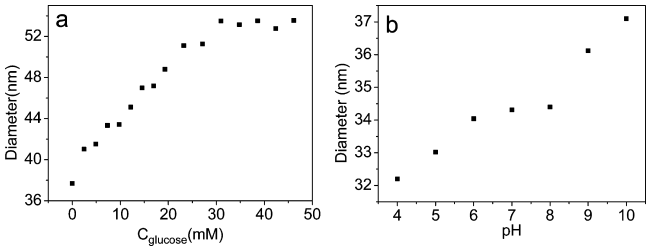

Figure 2. Average diameter of Ag@PAPBA-PAA hybrid nanoparticles as tuned by (a) various glucose concentrations and (b) pH values.

average size of the Ag@PAPBA-PAA hybrid nanoparticles gradually increased upon addition of glucose to the aqueous nanoparticle dispersion in a PBS buffer of pH of 9.0. The initial average size of the Ag@PAPBA-PAA hybrid nanoparticles is only about 38 nm without addition of glucose; however, the average size can increase up to 53 nm with a swelling about 40%. It is interesting that the size versus glucose concentration plot flattens off when the glucose concentration is above 30 mM, indicating that the PAPBA-PAA shell reaches a maximum swelling and then shows a less sensitive response to any further increase in glucose concentration.

The Ag@PAPBA-PAA hybrid nanoparticles are not only glucose-responsive, but also pH-responsive because PAA is known to be sensitive to pH, whereby polymer chains tend to be negatively charged and swell in water as the pH is increased. In the experiments, the pH-dependence experiments were performed in an aqueous solution without glucose to study the influence of pH. It can be seen from Figure 2b that with an increase in pH, the average particle size exhibits an increase in the pH range of 4 to 6, in which pH-responsive swelling may be attributed to the gradual ionization of carboxylic groups on the PAA backbone. In the pH range of 6−8, the PAA moieties adopt an ionized state and the APBA groups remain uncharged. The nanoparticle diameter stays at a stable level in this range, indicating that there is no obvious change in the charge density of the hybrid nanoparticles that can influence the swelling behavior.

When the pH is further increased to above 8, the APBA groups can bind one hydroxyl ion to form a charged state, which will greatly increase the charge repulsion, resulting in a dramatic swelling of the Ag@PAPBA-PAA hybrid nanoparticles. In this case, the hybrid nanoparticles can show a sensitive response to alteration of pH. The PAPBA-PAA shells shrink when the pH becomes low, resulting in a decrease in size; otherwise, the polymeric shells swell and the sizes increase. The situation contrasts with that of glucose control in that the sizes of the nanoparticles can be tuned to be smaller than the initial size at low pH, a phenomenon that allows us to shrink the prepared hybrid nanoparticles. It should be emphasized that for these Ag@PAPBA-PAA hybrid nanoparticles, both glucose response and pH response can ensure a good shell thickness control, which provides us with the opportunity to precisely tune the distance between the Ag nanoparticles and fluorophores for the controlled MEF studies.

Because their distance-dependent nature, MEF effects can be efficiently tuned by varying the thickness of the interlayer with external stimuli. In this work, the unique properties of controllable shell thickness enable the Ag@PAPBA-PAA hybrid nanoparticles to be good candidates to realize a tunable MEF behavior. By varying the glucose concentration or the pH of the

environment, we can control the average distance between Ag nanoparticles and adsorbed Por^{4+} entities.

Figure 3 shows that the MEF effect of Por^{4+}/Ag@PAPBA-PAA hybrid nanocomposites can be tuned by the alteration of

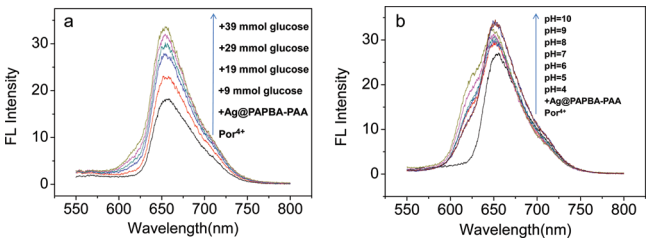

Figure 3. Fluorescence spectra of the Por^{4+}/Ag@PAPBA-PAA nanocomposite as tuned by (a) various glucose concentrations and (b) pH of the environment.

glucose concentration or pH value. It is clearly shown in Figure 3a that the fluorescence intensity of the nanocomposite is enhanced with an increase in glucose concentration and remains relatively insensitive to further increases in concentration after a 1.8-fold enhancement is reached. As mentioned above, the PAPBA-PAA shell of the hybrid nanoparticles swell when binding with glucose molecules, and the average distances between the Ag core and Por^{4+} molecules are increased. Since the MEF effect greatly depends on the interaction distance between the dye and the metal substrate, and normally the optimal distance is between 5 and 20 nm,[5] the fluorescence intensity of the Por^{4+} is tuned by the glucose and pH control of the PAPBA-PAA shell thickness. When the distances are enlarged beyond the most effective distances, the enhancement of the fluorescence intensity does not occur. So by varying the pH of the environment, the fluorescence intensity displayed by the nanocomposite has been enhanced via the shell swelling of Ag@PAPBA-PAA hybrid nanoparticles.

For further studies of tunable MEF effects, the plots of MEF effects (represented by I/I_0, where I_0 is the fluorescence intensity of pure Por^{4+} solution without the addition of Ag@PAPBA-PAA nanoparticles at same experimental conditions) and average size of the nanoparticles at 25 °C are shown in panels a and b in Figure 4. The average size of the core−shell nanoparticles changes from 38 to 53 nm with an increase in glucose concentration from 0 to 39 mM, which indicated that, as the average size of the Ag cores is 23 nm, the average distance between Ag cores and Por^{4+} entities has been increased from 7.5 to 15.0 nm. At the same time, the fluorescence intensity enhancement ratio I/I_0 increases from 1.3 to 1.8 with the glucose-responsive swelling of the PAPBA-PAA shell. As the hybrid nanoparticles with a shell thickness of about 28.5 nm showed almost no enhancement, we can also know that a thickness of 15 nm described in the manuscript is quite close to the optimal distance of MEF effects in this hybrid nanoparticles system.

Similar results were obtained in pH tuning experiments. In a pH range of 4−10, the average size increases with an increase in pH value, as does the fluorescence intensity, which indicates that the nanoparticles shrink when the pH is reduced and swell when the pH is increased, as shown in panels c and d in Figure 4. It is also found that the MEF enhancements show a relationship with the shell thickness of the hybrid nanoparticles, indicating that the MEF effects in this system increase with the swelling of the PAPBA-PAA shell until the thickness reaches a

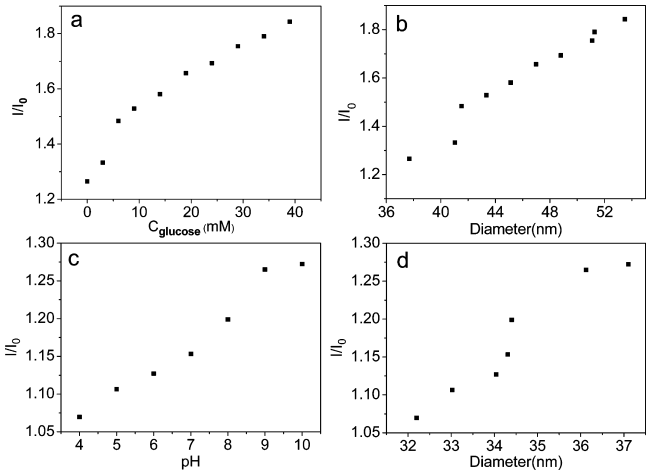

Figure 4. (a) Glucose-responsive MEF effects of the Por^{4+}/Ag@PAPBA-PAA nanocomposite as tuned by glucose concentration and (b) the plots of the MEF enhancements and the nanoparticle sizes. (c) MEF effects of the Por^{4+}/Ag@PAPBA-PAA nanocomposite as tuned by pH and (d) the plots of the MEF enhancements and the nanoparticle sizes.

maximum of about 15.0 nm at high glucose concentration. At a low pH such as 4, the PAPBA-PAA shell adopts a shrinkage state due to the strong hydrogen bonding between carboxylic groups and boronic acid groups. This induces the decrease in MEF enhancement. The mild change of the fluorescence to pH is corresponding to the size change with the decreasing pH, indicating the distance tuning is the main reason for the responsive MEF effects. Moreover, we have confirmed that the Por^{4+} can exhibit a stable fluorescence in the pH range of 2−12 in controlled experiments. This indicates that the Por^{4+} is not so pH-sensitive and the change on fluorescence intensity is mainly attributed to the responsive MEF effects. By simply tuning the pH or glucose concentration of the environment, the MEF of the nanocomposite can be effectively controlled.

CONCLUSION

In summary, a type of novel size-tunable hybrid core−shell nanoparticle system was synthesized by coating the Ag cores with glucose- and pH-responsive PAPBA-PAA shells. By tuning the glucose concentration or the pH of the environment, the hybrid nanoparticles can exhibit a sensitive swelling−shrinking behavior, which shows a size enlargement of about 40%. At the same time, because of the controllable shell thickness of the hybrid particle, the average distance between the Ag cores and the Por^{4+} molecules can be simply tuned, which resulted in a glucose- and pH-responsive MEF effect of the nanocomposite due to its interaction distance-dependent nature. To further obtain much higher surface plasmon resonance efficiency and better biocompatibility, we are now undertaking the preparation of hybrid nanoparticles with irregular Ag and Au cores and corresponding MEF experiments. It is confidently anticipated that this research can provide new approaches in the area of responsive detection and sensing.

AUTHOR INFORMATION

Corresponding Author

*E-mail: lidong@mater.ustb.edu.cn (L.L); nma@ustb.edu.cn (N.M.).

Notes

The authors declare no competing financial interest.

■ ACKNOWLEDGMENTS

This work was financially supported by the National Natural Science Foundation of China (20904003, 90923015, 21104004), the Doctoral Fund of the Ministry of Education of China (20110006120001), and the Fundamental Research Funds for the Central Universities of China.

■ REFERENCES

(1) Liu, B.; Bazan, G. C. *Chem. Mater.* **2004**, *16*, 4467.
(2) Thomas, S. W. III; Joly, G. D.; Swager, T. M. *Chem. Rev.* **2007**, *107*, 1339.
(3) Duan, X.; Liu, L.; Feng, F.; Wang, S. *Acc. Chem. Res.* **2010**, *43*, 260.
(4) Parthasarathy, A.; Ahn, H.-Y.; Belfield, K. D.; Schanze, K. S. *ACS Appl. Mater. Interfaces* **2010**, *2*, 2744.
(5) Lakowicz, J. R. *Anal. Biochem.* **2001**, *298*, 1.
(6) Geddes, C. D.; Parfenov, A.; Roll, D.; Gryczynski, I.; Malicka, J.; Lakowicz, J. R. *J. Fluoresc.* **2003**, *13*, 267.
(7) Aslan, K.; Huang, J.; Wilson, G. M.; Geddes, C. D. *J. Am. Chem. Soc.* **2006**, *128*, 4206.
(8) Yamaguchi, T.; Kaya, T.; Takei, H. *Anal. Biochem.* **2007**, *364*, 171.
(9) Aslan, K.; Malyn, S. N.; Geddes, C. D. *Biochem. Biophys. Res. Commun.* **2006**, *348*, 612.
(10) Li, Z.; Lou, X.; Li, Z.; Qin, J. *ACS Appl. Mater. Interfaces* **2009**, *1*, 232.
(11) Leong, K.; Zin, M. T.; Ma, H.; Sarikaya, M.; Huang, F.; Jen, A. K.-Y. *ACS Appl. Mater. Interfaces* **2010**, *2*, 3153.
(12) Qiu, T.; Jiang, J.; Zhang, W.; Lang, X.; Yu, X.; Chu, P. K. *ACS Appl. Mater. Interfaces* **2010**, *2*, 2465.
(13) Aslan, K.; Wu, M.; Lakowicz, J. R.; Geddes, C. D. *J. Am. Chem. Soc.* **2007**, *129*, 1524.
(14) Tang, F.; He, F.; Cheng, H.; Li, L. *Langmuir* **2010**, *26*, 11774.
(15) Tang, F.; Ma, N.; Wang, X.; He, F.; Li, L. *J. Mater. Chem.* **2011**, *21*, 16943.
(16) Tang, F.; Ma, N.; Tong, L.; He, F.; Li, L. *Langmuir* **2012**, *28*, 883.
(17) Wang, X.; He, F.; Tang, F.; Ma, N.; Li, L. *Colloids Surf., A* **2011**, *392*, 103.
(18) Ray, K.; Badugu, R.; Lakowicz, J. R. *Chem. Mater.* **2007**, *19*, 5902.
(19) dos Santos, D. S. Jr.; Aroca, R. F. *Analyst* **2007**, *132*, 450.
(20) Wang, Y.; Liu, B.; Mikhailovsky, A.; Bazan, G. C. *Adv. Mater.* **2010**, *22*, 656.
(21) Ma, N.; Tang, F.; Wang, X.; He, F.; Li, L. *Macromol. Rapid Commun.* **2011**, *32*, 587.
(22) Cheng, D.; Xu, Q. *Chem. Commun.* **2007**, 248.
(23) Li, Y.; Guan, L.; Zhang, H.; Chen, J.; Lin, S.; Ma, Z.; Zhao, Y. *Anal. Chem.* **2011**, *83*, 4103.
(24) Wang, L.; Liu, M. Z.; Gao, C. M.; Ma, L. W.; Cui, D. P. *React. Funct. Polym.* **2010**, *70*, 159.
(25) Asher, S. A.; Alexeev, V. L.; Goponenko, A. V.; Sharma, A. C.; Lednev, I. K.; Wilcox, C. S.; Finegold, D. N. *J. Am. Chem. Soc.* **2003**, *125*, 3322.
(26) Sivaraman, S. K.; Elango, I.; Kumar, S.; Santhanam, V. *Curr. Sci.* **2009**, *97*, 1055.
(27) Zhang, Y.; Guan, Y.; Zhou, S. *Biomacromolecules* **2007**, *8*, 3842.
(28) Zhang, Y.; Guan, Y.; Zhou, S. *Biomacromolecules* **2006**, *7*, 3196.